Talanta 120 (2014) 318–324

Contents lists available at ScienceDirect

Talanta

journal homepage: www.elsevier.com/locate/talanta

Development of molecular imprinted nanosensor for determination of tobramycin in pharmaceuticals and foods

Mehmet Lütfi Yola [a,b], Lokman Uzun [c,*], Nuran Özaltın [b], Adil Denizli [c]

[a] Sinop University, Faculty of Science, Department of Chemistry, Sinop, Turkey
[b] Hacettepe University, Faculty of Pharmacy, Department of Analytical Chemistry, Ankara, Turkey
[c] Hacettepe University, Faculty of Science, Department of Chemistry, Ankara, Turkey

ARTICLE INFO

Article history:
Received 30 July 2013
Received in revised form
28 October 2013
Accepted 31 October 2013
Available online 1 December 2013

Keywords:
Tobramycin
QCM
Molecular imprinting
Validation
Nanosensor

ABSTRACT

In this study, we developed quartz crystal microbalance (QCM) nanosensor for the real-time detection of tobramycin (TOB). Firstly, the modification of gold surface of QCM chip was performed by self-assembling monolayer formation of allyl mercaptane to introduce polymerizable double bonds on the chip surface. Then, TOB imprinted poly(2-hydroxyethyl methacrylate–methacryloylamidoglutamic acid) [p(HEMA–MAGA)] film was generated on the gold surface. The nonmodified and TOB-imprinted p(HEMA–MAGA) surfaces were characterized by using atomic force microscopy (AFM), Fourier transform infrared (FTIR) spectroscopy, ellipsometry and contact angle measurements. The proposed method was validated according to the ICH guideline. The linearity range and the detection limit (S/N=3) were obtained as 1.7×10^{-11}–1.5×10^{-10} M and 5.7×10^{-12} M, respectively. The developed method was applied to pharmaceuticals, and food samples such as chicken egg white and milk extract for the determination of TOB. In addition, association kinetics analysis and isotherm models were applied to the data to explain the adsorption process that took place.

1. Introduction

Tobramycin (Scheme 1) is an aminoglycoside (AG) antibiotic which is composed of amino sugars linked by glycosidic bonds to an aminocyclitol named 2-desoxystreptamine [1]. AG drugs are utilized to treat the infections caused by aerobic Gram-negative and some Gram-positive microorganisms [2]. However, the use of large amount of the AGs may result in the effects of ototoxicity and nephrotoxicity. Hence, the monitoring of the drug in the metabolism of patients is important. Tobramycin is a water-soluble AG antibiotic. It is obtained from the fermentation of the actinomycete *Streptomyces tenebrarius* and used in a variety of pharmaceuticals such as TobraDex® and TOBI® [3]. Various analytical methods such as chromatography have been developed for determination of AGs [4], including thin-layer chromatography [5], gas chromatography [6], liquid chromatography [7,8], liquid chromatography–mass spectrometry [9,10], and capillary zone electrophoresis [11,12]. But these methods have some disadvantages such as large material consumption, personnel skill, and expensive equipment.

QCM calculates the changes of mass on quartz crystal surface by measuring its difference of frequency in real time [13]. The QCM technique is a selective, simple and sensitive method [14], which has been utilized for the determination of clinical targets [15], environmental pollutants [14,16], oxidative stress [17,18], some proteins [19] and investigation of bimolecular interactions [20].

Although various methods are used to generate the sensitive QCM sensor, the most effective method is the molecular imprinting technique. The method relies on the molecular recognition. It is a kind of polymerization which is formed around the target molecule. Hence this technique forms specific cavities in the cross-linked polymeric matrices [21]. Molecular imprinted polymers (MIPs) have various applications such as artificial enzymes [21], solid-phase extraction [22], bioseparation [23,24], affinity detoxification [25] and sensor devices [26–30].

In this study, we prepared TOB-imprinted p(HEMA–MAGA) film on gold surface of QCM chip. The developed nonmodified and modified surfaces were characterized by using AFM, FTIR, ellipsometry and contact angle measurements. After that, the developed nanosensor was applied to some real samples for the determination of TOB spiked.

2. Experimental

2.1. Materials

TOB, kanamycin A (KAN-A), amikacin (AMIK) and gentamycin (GEN) were purchased from Fargem Company (Düzce, Turkey) and

* Corresponding author. Tel.: +90 312 2977337; fax: +90 312 2992163.
E-mail address: lokman@hacettepe.edu.tr (L. Uzun).

0039-9140/$ - see front matter © 2013 Elsevier B.V. All rights reserved.
http://dx.doi.org/10.1016/j.talanta.2013.10.064

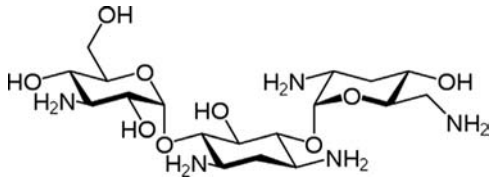

Scheme 1. Chemical structure of TOB.

used as received. The stock solution of TOB (1.0 mM) was prepared by dissolving it in 20 mL of ultra-pure quality water and then diluting it with ultra-pure quality water to 50 mL. The working solutions were prepared by diluting the stock solution with 0.10 M phosphate buffer (pH 7.5). Allyl mercaptane (CH_2CHCH_2SH), HEMA, ethylene glycol dimethacrylate (EGDMA), N,N′-azobisisobutyronitrile (AIBN), trichloroacetic acid (TCA) and sodium chloride (NaCl) were obtained from Sigma-Aldrich. MAGA was obtained from Nanoreg Ltd. Şti., Ankara, Turkey. The other chemicals were used as received.

2.2. Surface modification of the QCM chips

2.2.1. Allyl mercaptane modification of QCM chip

To modify gold surface of the QCM chip with CH_2CHCH_2SH, the chip was washed with alkaline piranha solution (3:1 NH_4OH:H_2O_2, v/v). After the QCM chip was dipped in 10 mL of cleaning solution for 5 min, it was washed with ethyl alcohol and dried in a vacuum oven (200 mmHg, 35 °C) for 2 h. To let vinyl groups into the gold surface, the chip was dipped in an ethanol/water (4:1, v/v) solution containing 3.0 M CH_2CHCH_2SH and allowed to form self-assembled monolayer for 24 h. Then, it was cleaned with ethyl alcohol and dried with nitrogen gas.

2.2.2. Polymer preparation on QCM chip surface

TOB-imprinted p(HEMA–MAGA) film on CH_2CHCH_2SH modified QCM chip was prepared according to this protocol. Firstly, 2.33×10^{-6} mol of TOB and 4.65×10^{-6} mol of MAGA monomer were mixed with 500 μL of phosphate buffer (pH 7.5) at room temperature for 2 h. MAGA–TOB molar ratio was 2:1. After that, 5.0 mg of AIBN as initiator was dissolved in 1250 μL of HEMA and 500 μL of EGDMA and 200 μL of MAGA–TOB complex was added into this solution to prepare stock monomer solution. The solutions were passed with nitrogen gas for 15 min. Then, 20 μL of aliquot was taken from the stock monomer solution and dropped onto the QCM chip surface by using the *spin coating method*. The method is used to deposit uniform thin films to QCM surface. After 10 s, the QCM chip was removed from the spin coater and polymerization was started by UV light (100 W, 365 nm). After 60 min, polymer coated QCM chip was washed with ethanol three times, and then dried in a vacuum oven.

2.3. TOB removal from QCM chip surface

There are electrostatic interactions and hydrogen bonding between the carboxylic acid groups of MAGA monomer and polar groups of TOB molecules. In order to break the interactions, we used 1.0 M NaCl solution in water as a desorption agent. Firstly, the removal study of TOB was performed via a batch system. TOB-imprinted p(HEMA–MAGA) surface was dipped into 25 mL of desorption agent. The QCM chip was washed in a bath (200 rpm) at room temperature. After TOB removal, the QCM chip was washed with ultra-pure quality water and dried with nitrogen gas under vacuum (200 mmHg, 25 °C).

2.4. Characterization methods

The contact angle of the surfaces was obtained with a KRUSS DSA100 (Hamburg, Germany) instrument. Contact angles were measured with the Sessile Drop method by dropping one water drop. Ten photos were obtained from different parts of QCM chips. The calculated values for the QCM surfaces were the mean of the 10 measurements.

In order to characterize the surfaces, tapping mode AFM was used (Nano Magnetics Instruments, Oxford, UK). QCM chip was installed on a sample holder. $2\ \mu m \times 2\ \mu m$ sample area was showed with a 128×128 pixels resolution. The scan rate was $2\ \mu m\ s^{-1}$. The studies were performed in air atmosphere.

Ellipsometer measurements were also performed by using an auto-nulling imaging ellipsometer (Nanofilm EP3, Germany) to characterize the surface of QCM chips. The measurements have been carried out at a wavelength of 532 nm with an angle of incidence of 72°. In the layer thickness analysis, a four-zone auto-nulling procedure integrating over a sample area of $\sim 50 \times 50\ \mu m^2$ followed by a fitting algorithm has been performed. The measurements were performed at six different points of the QCM chip and the results were obtained as the mean value.

For FTIR measurements, TOB-imprinted p(HEMA–MAGA) nanosensor was put into a sample holder of a FTIR spectrophotometer (Thermo Fisher Scientific, Nicolet iS10, Waltham, MA, USA). The spectra were obtained in the wave number range of 650–4000 cm^{-1} with 2 cm^{-1} resolution.

2.5. Pharmaceuticals and sample preparation

The pharmaceutical eye drops were dissolved in phosphate buffer (pH 7.5) to obtain a concentration level within the linearity range and filtrated by a 0.45-μm syringe filter. The pharmaceutical preparations were done as the following.

TOBRADEX® contains 3.0 mg/mL TOB, 1.0 mg/mL dexamethasone and 0.01% benzalkonium chloride as preservative. TOBI® contains 60 mg/mL TOB and 11.25 mg NaCl. In addition, synthetic preparations were prepared by mixing excipients and labeled amounts (3.0 mg and 60 mg) of TOB. Then, the mixture was transferred to a 50-mL volumetric flask.

The two different food samples such as chicken egg and milk were bought from local supermarket. The extraction and dilution procedures of the samples were as follows: 5.0 mL of milk sample was mixed with 1.0 mL of TCA (10% m/v) by a vortex mixer for 25 s and centrifuged at 4500 rpm for 15 min. The supernatant was transferred to another centrifuge tube and the precipitate was treated twice as mentioned above. The collected supernatant was centrifuged again at 4500 rpm for 5 min and filtrated by a 0.45-μm syringe filter. The filtrate was directly used as the sample solution. The filtrate was diluted with phosphate buffer (pH 7.5) for analysis.

Chicken egg white was efficiently stored at −20 °C. 1.0 g samples and 10 mL of phosphate buffer (pH 7.5) were mixed for 2 min and centrifuged at 4500 rpm for 15 min. The supernatant liquid was diluted with phosphate buffer (pH 7.5) for analysis.

2.6. Procedure of the analysis

The real time determination of TOB was performed using a QCM system (RQCM, INFICON Acquires Maxtek, NY, USA) in an insulation cabinet (Supplementary materials, Fig. SM1) for avoiding temperature and pressure fluctuation effect on the sensor response. After the TOB-imprinted p(HEMA–MAGA) surface was washed with ultra-pure quality water (5.0 mL) with 1.0 mL min^{-1} of flow-rate, pH 7.5 of phosphate buffer (5.0 mL) (1.0 mL min^{-1} of flow-rate) was applied to obtain the steady resonance frequency

(f_0). After that, TOB solutions with different concentrations in 0.1 M phosphate buffer (pH 7.5) (5 mL) were applied to the QCM system (1.0 mL min^{-1} of flow-rate). Frequency shifts were monitored and evaluated via software supplied by manner fracture. The desorption studies were carried out using 1.0 M NaCl solution (5.0 mL) with 1.0 mL min^{-1} of flow-rate. After that, the TOB imprinted QCM chip was washed with ultra-pure quality water and 0.1 M phosphate buffer (pH 7.5). The steps of adsorption–desorption–regeneration were repeated for each TOB concentration.

3. Results and discussion

3.1. Characterization of TOB imprinted QCM nanosensor

TOB-imprinted p(HEMA–MAGA) film QCM nanosensor was characterized by using FTIR spectroscopy, AFM, ellipsometry and contact angle. Before TOB removal from QCM chip surface, the specific bands of the polymeric structure such as O–H stretching of TOB at 3310 cm^{-1}, saturated C–H stretching of TOB at 2918 cm^{-1}, carboxyl–carbonyl stretching at 1738 cm^{-1} and amide–carbonyl absorption at 1621 cm^{-1} have been observed in Fig. 1A. In addition, N–H bonding peak at 1540 cm^{-1} corresponded to amide vibration of MAGA. The characteristic frequencies for C–H groups at 1375–1429 cm^{-1} result from bonding vibration in the template molecule (TOB).

The measurement of ellipsometry was also performed and the harmony between AFM and ellipsometry is clear. The surface deepness of TOB imprinted QCM nanosensor is 12.80 ± 1.40 nm (Fig. 1B). Hence we can say that a homogeneous and monolayer film formation has been achieved.

As seen in Fig. 1C, contact angle values of unmodified and allyl mercaptane modified QCM surfaces were obtained as 79.14 ± 1.48 and 70.34 ± 2.04, respectively. The decrease in surface contact angles indicated that hydrophilicity or polarity of surface increased. The contact angle value of TOB-imprinted p(HEMA–MAGA) film on CH_2CHCH_2SH modified QCM chip was obtained as 63.22 ± 3.12. The increase of hydrophilic character of surface is expected due to the hydrophilic structure of MAGA monomer containing two carboxylic acid groups.

AFM images of QCM surfaces were obtained in noncontact mode (Fig. 1D). The values of surface deepness for unmodified, CH_2CHCH_2SH modified and TOB-imprinted p(HEMA–MAGA) film on CH_2CHCH_2SH modified QCM chips are 2.48 ± 0.45, 7.10 ± 1.17 and 16.9 ± 2.07 nm, respectively. These results indicate that allyl mercaptane modification of QCM chip was achieved homogeneously. In addition, the surface deepness of the TOB-imprinted p(HEMA–MAGA) film increased. This result confirmed that polymerization could be accomplished on the QCM chip.

3.2. Validation for proposed QCM method

3.2.1. Effect of pH

A series of 0.10 M phosphate buffer with different pH was tested in the presence of 0.054 nM TOB. The binding to QCM surface increases gradually up to pH 7.5. This situation is related to the structure of MAGA monomer. MAGA monomer is based on glutamic acid and has two pKa values (pKa1: 2.10, pKa2: 4.07). The increase in pH value caused the carboxylic acid groups of MAGA monomer to load negatively. These negative groups interacted efficiently with –OH groups of TOB. Hence, the affinity of sensor–analyte increased. When pH exceeds 7.5, the concentration of the anion form of TOB increases. Hence the binding to QCM

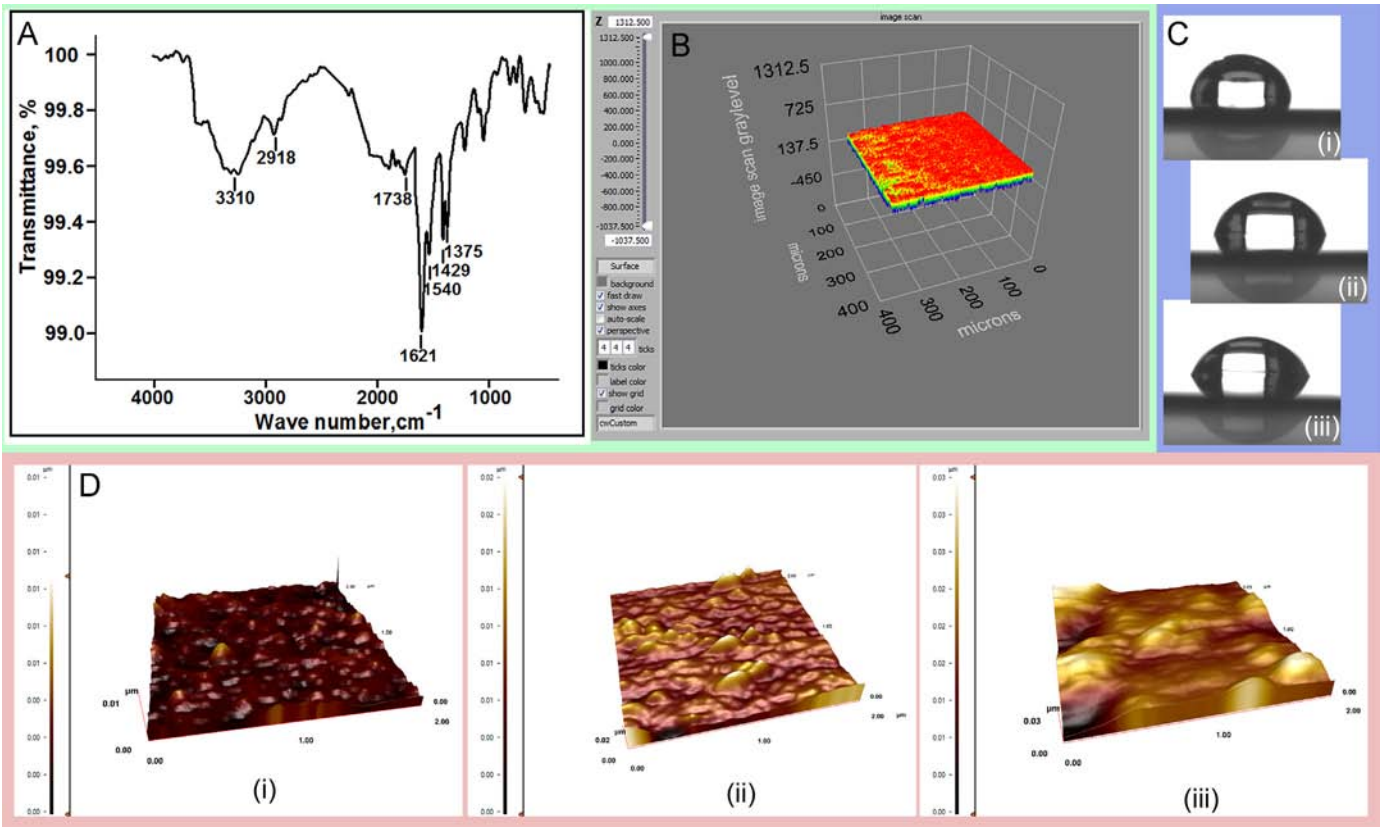

Fig. 1. (A) FTIR spectra of the TOB imprinted p(HEMA–MAGA); (B) ellipsometry image of TOB imprinted QCM nanosensor; (C) contact angles measurements of (i) nonmodified; (ii) CH_2CHCH_2SH modified; (iii) TOB imprinted p(HEMA–MAGA) film on QCM chip; and (D) AFM images of (i) nonmodified; (ii) CH_2CHCH_2SH modified; (iii) TOB imprinted p(HEMA–MAGA) film on QCM chip.

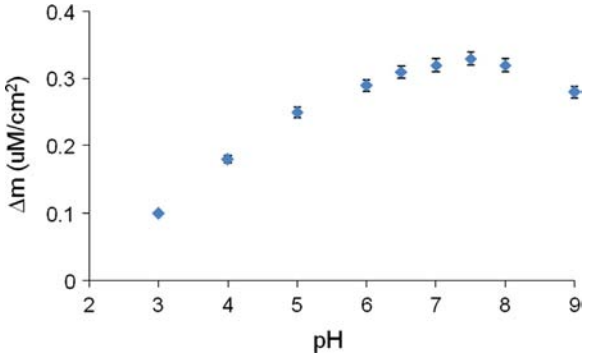

Fig. 2. Effect of pH on QCM response of TOB imprinted nanosensor.

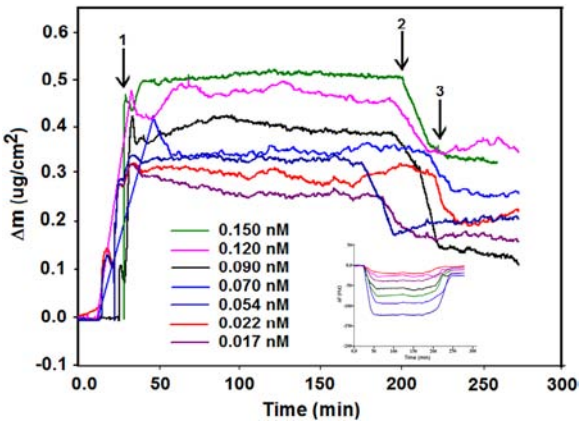

Fig. 3. Effect of concentration on QCM response of TOB imprinted nanosensor (1) adsorption, (2) desorption, and (3) regeneration. (Inset) frequency shift vs. time relation depending on concentration.

surface could be difficult. Hence, pH 7.5 was selected as optimum pH (Fig. 2).

3.2.2. Stability of TOB

The stock solutions of TOB were hidden at two different temperatures such as 4 °C for 20 days (long-term stability) and 25 °C for 24 h (short-term stability). The QCM responses were obtained and no important differences were found in TOB concentrations. These results indicate that TOB is highly stable.

3.2.3. Linearity range

The sensorgrams with increasing TOB concentration (Fig. 3) demonstrate that the mass shift increased linearly with concentration. Data of the calibration curves are given in Table 1. As clearly seen in Fig. 3, the QCM response was gradually measured in respect to increase in TOB concentration. This situation is directly related to basic adsorption phenomena which describes concentration difference between liquid and solid phases. These phases drive analyte molecules through the surface to interact with specific ligands/cavities. It should be mentioned here, the correlation between frequency shift and mass accumulation on the surface is clearly seen in this figure (inset shows frequency shift vs. time relation for the sensor).

3.2.4. Precision and accuracy

Three different concentrations of TOB (0.022, 0.070 and 0.120 nM) in the linear range were evaluated in six independent series on the same day and six consecutive days. The relative standard deviation (RSD) values changed from 1.25 to 2.27 for intraday and from 1.25 to 3.18 for interday precision. The low RSD values showed that the proposed method has good precision [31]. In addition, both results obtained for intraday and interday accuracy (bias) were $\leq 3.00\%$ [31].

3.2.5. Recovery

In order to evaluate the effect of excipients on the proposed method, synthetic tablet solutions were prepared as mentioned in Section 2 and analyzed by the developed method. The recovery values are between 98.22% and 102.43% with RSD < 2.00. In addition, the recovery values for milk and egg samples are presented in Table 2. Closeness of the results to 100.00% showed that recovery of the method was very good for pharmaceuticals (TOBRADEX® and TOBİ®) and food samples.

3.2.6. Selectivity of TOB-imprinted QCM nanosensor

The sensorgrams of drug solutions and synthetic preparations were identical with sensorgrams of standard solutions containing 0.054 nM TOB (Fig. 4A and B). In addition, to confirm the selectivity of the TOB imprinted QCM nanosensor against TOB in milk and egg samples in the presence of KAN-A, AMIK and GEN as competitors (Fig. 4C), the samples were applied to the nanosensors. The selectivity coefficients (k) and relative selectivity coefficients (k') values are given in Table 3. TOB imprinted QCM nanosensor was 10.0, 12.0 and 11.11 times more selective for TOB than GEN, AMIK and KAN-A, respectively. The results show that because of selective cavities in the polymer structure, TOB imprinted QCM nanosensor has higher adsorption capacity (Δm values) for TOB in comparison to GEN, AMIK and KAN-A. To display the specificity of TOB imprinted QCM nanosensor, non-imprinted QCM nanosensor (NIP) was also prepared and the signals of nonimprinted QCM nanosensor to TOB, GEN, AMIK and KAN-A were obtained as 0.024, 0.022, 0.030 and 0.023 $\mu g\ cm^{-2}$, respectively (Fig. 4D). The selectivity coefficients for nonimprinted QCM nanosensor in respect to GEN, AMIK, and KAN-A were calculated as 1.1, 0.8, and 1.2, respectively. The results for relative selectivity constants showing selectivity gained by imprinting process display that TOB imprinted QCM nanosensor was 9.1,

Table 1
Data of the calibration curves for the proposed methods ($n=7$).

Regression equation	$y=2.785x+0.211$[a]
Standard error of slope	0.54
Standard error of intercept	0.37
Correlation coefficient (r)	0.9985
Linearity range (nM)	0.017–0.150
LOD (nM)	0.006
LOQ (nM)	0.017

[a] $y=ax+b$; y, mass shift ($\mu g\ cm^{-2}$); x, TOB concentration (nM); a, slope; b, intercept; LOD, limit of detection; and LOQ, limit of quantification.

Table 2
The recoveries of TOB in milk and egg samples ($n=7$).

Sample	Added TOB (M)	Found TOB (M)	Recovery (%)
Milk	–	$4.12(\pm 0.04)\times 10^{-11}$	–
	1.0×10^{-11}	$5.03(\pm 0.01)\times 10^{-11}$	98 ± 3
	4.0×10^{-11}	$7.98(\pm 0.04)\times 10^{-11}$	98 ± 2
	6.0×10^{-11}	$9.80(\pm 0.06)\times 10^{-11}$	97 ± 2
Egg white	–	$8.42(\pm 0.07)\times 10^{-11}$	–
	1.0×10^{-11}	$9.14(\pm 0.03)\times 10^{-11}$	97 ± 2
	4.0×10^{-11}	$11.91(\pm 0.03)\times 10^{-11}$	96 ± 3
	6.0×10^{-11}	$14.07(\pm 0.02)\times 10^{-11}$	98 ± 3

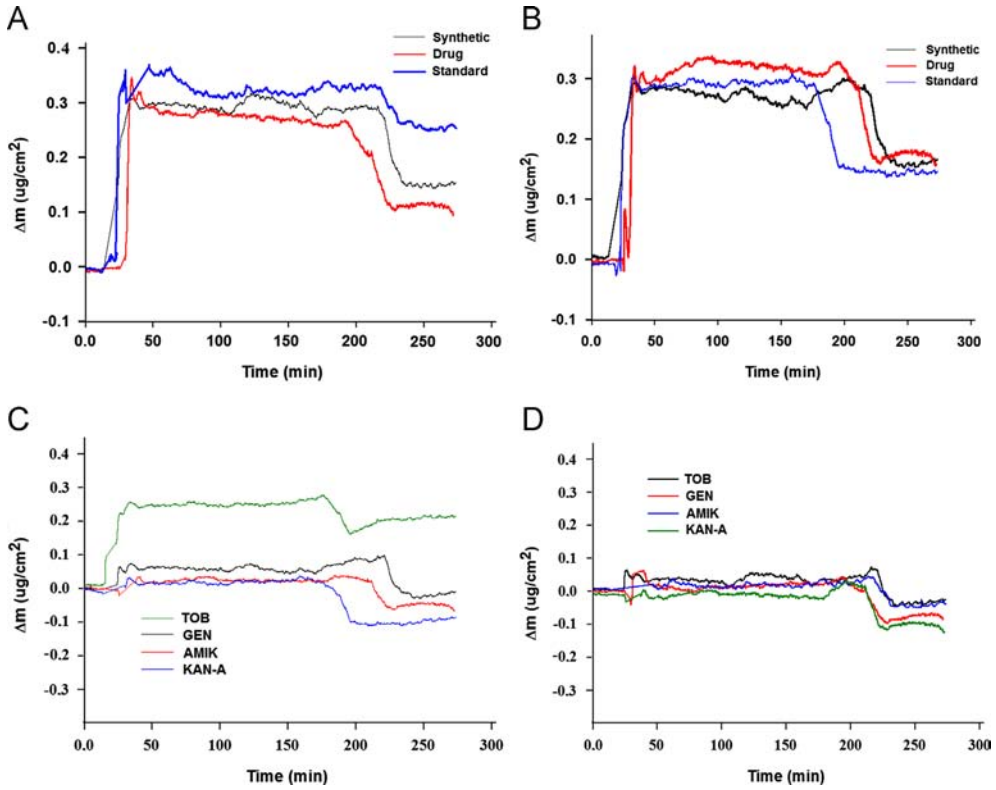

Fig. 4. Comparison of selectivity of QCM sensors. The QCM responses of (A) synthetic preparation, tablet and standard solution (0.054 nM TOB) for TOBRADEX® on TOB imprinted nanosensor; (B) synthetic preparation, tablet and standard solution (0.054 nM TOB) for TOBİ® on TOB imprinted nanosensor; (C) TOB, GEN, AMIK and KAN-A (each of 0.054 nM) on TOB imprinted nanosensor; and (D) TOB, GEN, AMIK and KAN-A (each of 0.054 nM) on nonimprinted QCM sensor.

Table 3
The selectivity coefficients (k) and relative selectivity coefficients (k') values of TOB imprinted QCM nanosensor.

	MIP		NIP		k'
	Δm	k	Δm	k	
TOB	0.300	–	0.024	–	–
GEN	0.030	10.0	0.022	1.1	9.1
AMIK	0.025	12.0	0.030	0.8	15.0
KAN-A	0.027	11.11	0.020	1.2	9.3

15.0 and 9.3 times more selective in comparison to GEN, AMIK and KAN-A, respectively.

In addition, the regression equations of the standard addition curve for TOBRADEX®, TOBİ®, milk and egg were found to be $y=2.742x+7.814$, $y=2.803x+8.219$, $y=2.703x+9.477$ and $y=2.821x+10.841$, respectively. There was no important difference between slopes of calibration and standard addition curves. The results indicated that no interference occurred during QCM detection processes.

3.2.7. Ruggedness

The effect of QCM response of two different analysts for 0.054 nM TOB was investigated. The data were evaluated by the Wilcoxon test and there was no crucial difference between the results of the two analysts ($p > 0.05$). Hence, we can say that the developed QCM method is rugged.

3.2.8. Repeatability of the TOB imprinted QCM nanosensor

In order to show the repeatability of TOB imprinted QCM nanosensor, six equilibration–adsorption–regeneration cycles were repeated by 0.054 nM TOB. As seen in Fig. 5, TOB imprinted QCM nanosensor has demonstrated repeated mass shift during the cycles.

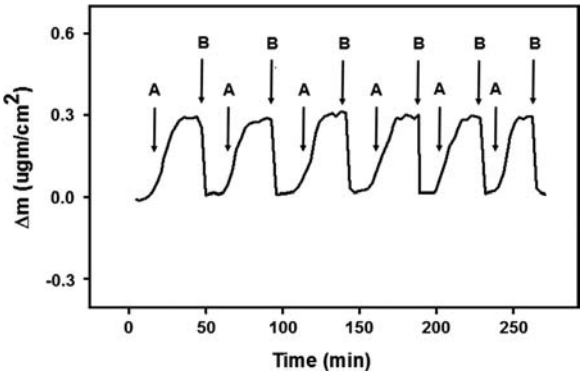

Fig. 5. Repeatability of TOB imprinted QCM nanosensor: (A) adsorption and (B) desorption.

3.2.9. Fabrication reproducibility and stability of the TOB imprinted QCM nanosensor

The fabrication reproducibility was evaluated with six different QCM chips that were prepared independently by the same procedure as in Section 2.2.2. The RSD is 0.88% for mass shift measuring in 0.054 nM TOB which demonstrates the reliability of the fabrication. In addition, the stability of TOB imprinted QCM nanosensor was also investigated. After 45 days, the value of mass shift is approximately 97.18% of the original value.

Table 4
Kinetic constants for the QCM method.

Equilibrium analysis (Scathard)		Association kinetics analysis	
Δm_{max} (μg cm^{-2})	0.5920	k_a (nM/s)	0.0003
K_A (nM)	38.01	k_d (s^{-1})	0.0040
K_D (nM^{-1})	0.0263	K_A (nM)	0.075
R^2	0.7750	K_D (nM^{-1})	13.33
		R^2	0.9330

Table 5
Langmuir, Freundlich and Langmuir–Freundlich constants for QCM method.

Langmuir		Freundlich		Langmuir–Freundlich	
Δm_{max}	0.5230	Δm_{max}	1.030	Δm_{max}	2.6860
K_A (nM)	55.56	$1/n$	0.3270	$1/n$	0.3270
K_D (nM^{-1})	0.018	R^2	0.9230	K_A (nM)	0.4360
R^2	0.9890			K_D (nM^{-1})	2.2930
				R^2	0.9590

3.3. Mathematical analysis of the TOB imprinted QCM nanosensor

QCM nanosensor data were analyzed for the determination of kinetic and equilibrium isotherm parameters such as forward and reverse binding constants, k_a (μg mL^{-1} s^{-1}) and k_d (s^{-1}), forward and reverse equilibrium constants, K_A (μg mL^{-1}) and K_D (mL μg^{-1}). For this purpose, pseudo-first-order kinetic analysis and four different equilibrium isotherm models, Scatchard, Langmuir, Freundlich, and Langmuir–Freundlich, were applied to the TOB imprinted QCM nanosensor data [29]. Linear form of applied model can be given as follows:

$$\text{Equilibrium kinetic analysis}: \ d\Delta m/dt = k_a C\Delta m_{max} - (k_a C + k_d)\Delta m \quad (1)$$

$$\text{Scathard}: \ \Delta m_{eq}/[C] = K_A(\Delta m_{max} - \Delta m_{eq}) \quad (2)$$

$$\text{Langmuir}: \ \Delta m = \{\Delta m_{max}[C]/(K_D + [C])\} \quad (3)$$

$$\text{Freundlich}: \ \Delta m = \Delta m_{max}[C]^{1/n} \quad (4)$$

$$\text{Langmuir} - \text{Freundlich}: \ \Delta m = \{\Delta m_{max}[C]^{1/n}/(K_D + [C]^{1/n})\} \quad (5)$$

where K_D is the equilibrium dissociation constant and $1/n$ is the Freundlich heterogeneity index. The Scatchard, Langmuir, Freundlich, and Langmuir–Freundlich isotherms were evaluated to investigate the interaction between TOB imprinted QCM nanosensor and TOB molecules (Tables 4 and 5). It was seen that the Langmuir isotherm was the best model (R^2=0.9890). According to the Langmuir model, a monolayer on a homogeneous surface is formed. The binding sites have the same adsorption affinity which is energetically [32]. Δm_{max} was calculated as 0.5230 μg cm^{-2}. This value is close to the experimental value (0.5450 μg cm^{-2}). K_A and K_D values were calculated as 55.56 nM and 0.018 nM^{-1}, respectively.

4. Conclusion

We developed QCM nanosensor for the determination of TOB in pharmaceuticals, milk and egg white samples. After the gold QCM surface was modified with allyl mercaptane, TOB-imprinted p(HEMA–MAGA) film was formed on the gold surface. The non-imprinted and TOB-imprinted p(HEMA–MAGA) surfaces were characterized by using AFM, FTIR, ellipsometry and contact angle measurements. According to the results, allyl mercaptane and TOB-imprinted p(HEMA–MAGA) modification of QCM chip were achieved homogeneously. In addition, a monolayer on a homogeneous surface is formed according to the Langmuir model. Hence a fast and simple nanosensor was prepared in this study which can offer new developments for detecting aminoglycoside antibiotics in the future.

Novelty statement

In the present work, we have combined the advantages of quartz crystal microbalance, molecular imprinting and pharmaceutical biosensor for real-time detection of tobramycin in food samples, egg and milk. For this aim, tobramycin molecules have been imprinted on polymeric nanofilms on the QCM sensor chip via the molecular imprinting approach. The coordination of template molecules have been achieved by using 2-hydroxyethyl methacrylate and N-methacryloyl-L-glutamic acid (polymerizable derivative of L-glutamic acid) as functional monomers whereas ethylenglycol dimethacrylate has been used as cross-linker. The nanosensor has been characterized by several methods, i.e. the Fourier transform infrared spectroscopy, ellipsometry, contact angle measurements, and atomic force microscopy. Tobramycin detection has been studied from aqueous solution to optimize working condition and calculate sensor parameters. It would be first report for the tobramycin detection with molecular imprinted QCM nanosensor.

Appendix. Supplementary material

Supplementary data associated with this article can be found in the online version at http://dx.doi.org/10.1016/j.talanta.2013.10.064.

References

[1] R. Oertel, V. Neumeister, W. Kirch, J. Chromatogr. A 1058 (2004) 197–201.
[2] J.G. Hardman, L.E. Limbird, The Pharmacological Basis of Therapeutics Goodman & Gilman's, New York, 2001.
[3] R. Edward, Physicians' Desk Reference PDR, 50th ed., Barnhart Publisher, Medical Economics Company Inc., Oradell, New Jersey, 1996.
[4] D.A. Stead, J. Chromatogr. B 747 (2000) 69–93.
[5] E. Roets, E. Adams, I.G. Muriithi, J. Hoogmartens, J. Chromatogr. A 696 (1995) 131–138.
[6] M. Preu, D. Guyot, M. Petz, J. Chromatogr. A 818 (1998) 95–108.
[7] S.H. Chen, Y.C. Liang, Y.W. Chou, J. Sep. Sci. 29 (2006) 607–612.
[8] J.M. Serrano, M. Silva, J. Chromatogr. B 843 (2006) 20–24.
[9] S. Bogialli, R. Curini, A. Di Corcia, A. Lagana, M. Mele, M. Nazzari, J. Chromatogr. A 1067 (2005) 93–100.
[10] D.N. Heller, J.O. Peggins, C.B. Nochetto, M.L. Smith, O.A. Chiesa, K. Moulton, J. Chromatogr. B 821 (2005) 22–30.
[11] C.Z. Yu, Y.Z. He, G.N. Fu, H.Y. Xie, W.E. Gan, J. Chromatogr. B 877 (2009) 333–338.
[12] W.S. Law, P. Kuban, L.L. Yuan, J.H. Zhao, S.F.Y. Li, P.C. Hauser, Electrophoresis 27 (2006) 1932–1938.
[13] K.A. Marx, Biomacromolecules 4 (2003) 1099–1120.
[14] S. Kurosawa, J.W. Park, H. Aizawa, S.I. Wakida, H. Tao, K. Ishihara, Biosens. Bioelectron. 22 (2006) 473–481.
[15] Y.A. Mao, W.Z. Wei, S.F. Zhang, G.M. Zeng, Anal. Bioanal. Chem. 373 (2002) 215–221.
[16] E. Ozgür, E. Yilmaz, G. Sener, L. Uzun, R. Say, A. Denizli, Environ. Prog. Sustain. Energy 32 (2013) 1164–1169.
[17] R. Say, A. Gultekin, A.A. Ozcan, A. Denizli, A. Ersoz, Anal. Chim. Acta 640 (2009) 82–86.
[18] A. Ersoz, S.E. Diltemiz, A.A. Ozcan, A. Denizli, R. Say, Sens. Actuators B: Chem. 137 (2009) 7–11.
[19] G. Sener, E. Ozgur, E. Yilmaz, L. Uzun, R. Say, A. Denizli, Biosens. Bioelectron. 26 (2010) 815–821.
[20] S. Svedhem, D. Dahlborg, J. Ekeroth, J. Kelly, F. Hook, J. Gold, Langmuir 19 (2003) 6730–6736.
[21] F. Bonini, S. Piletsky, A.P.F. Turner, A. Speghini, A. Bossi, Biosens. Bioelectron. 22 (2007) 2322–2328.
[22] C. Esen, M. Andac, N. Bereli, R. Say, E. Henden, A. Denizli, Mater. Sci. Eng. C Mater. Biol. Appl. 29 (2009) 2464–2470.
[23] L. Uzun, R. Say, S. Unal, A. Denizli, J. Chromatogr. B 877 (2009) 181–188.
[24] S. Asliyuce, L. Uzun, R. Say, A. Denizli, React. Funct. Polym. 73 (2013) 813–820.

[25] M. Andac, R. Say, A. Denizli, Molecular recognition based cadmium removal from human plasma, J. Chromatogr. B 811 (2004) 119–126.
[26] G. Sener, E. Ozgur, A.Y. Rad, L. Uzun, R. Say, A. Denizli, Analyst 138 (2013) 6422.
[27] V.K. Gupta, M.L. Yola, N. Ozaltin, N. Atar, Z. Ustundag, L. Uzun, Electrochim. Acta 112 (2013) 37–43.
[28] G. Erturk, L. Uzun, M.A. Tumer, R. Say, A. Denizli, Biosens. Bioelectron. 28 (2011) 97–104.
[29] L. Uzun, R. Say, S. Unal, A. Denizli, Biosens. Bioelectron. 24 (2009) 2878–2884.
[30] S.E. Diltemiz, D. Hur, A. Ersoz, A. Denizli, R. Say, Biosens. Bioelectron. 25 (2009) 599–603.
[31] J.M. Green, Anal. Chem. 68 (1996) A305–A309.
[32] S.K. Papageorgiou, F.K. Katsaros, E.P. Kouvelos, N.K. Kanellopoulos, J. Hazard. Mater. 162 (2009) 1347–1354.